

# Acta Scientifica Naturalis

Former Annual of Konstantin Preslavsky University – Chemistry, Physics, Biology, Geography  
Journal homepage: [asn.shu.bg](http://asn.shu.bg)

Received: 02.2019

Accepted: 03.2019

## Experimental setup for light-to-heat NIR conversion measurements of gold nanoparticle solutions

Nikolay Uzunov<sup>1,2</sup>, Michele Bello<sup>2,3</sup>, Laura Melendez-Alafort<sup>4</sup>, Laura De Nardo<sup>3,5</sup>

<sup>1</sup> “Konstantin Preslavsky” University of Shumen, Faculty of Natural Sciences, Department of Physics and Astronomy, 115 Universitetska Str., 9712, Shumen, Bulgaria

<sup>2</sup> National Laboratories of Legnaro (INFN), Viale dell’Università 2, 35020 Legnaro (Pd), Italy,

<sup>3</sup> Department of Physics and Astronomy, University of Padua, Via Marzolo 8, 35131 Padua, Italy,

<sup>4</sup> Veneto Institute of Oncology IOV – IRCCS, Via Gattamelata 64, Padua, Italy,

<sup>5</sup> National Institute for Nuclear Physics (INFN), Padua branch, Via Marzolo, 8, 35131 Padua, Ital

**Abstract:** *In recent years, there is a constantly increasing interest in the application of nanoparticles for cancer diagnosis and cancer therapy. In this respect, the most promising nano-objects at present are the gold nanoparticles. A very convenient and powerful property of these objects is their ability to increase their temperature under electro-magnetic irradiation with certain wavelength. In our research we have directed our efforts toward particular nano-objects specifically sensitive to electromagnetic radiation in the near-infrared region (NIR). In order to study the photothermic properties of the solutions of gold nanoparticles in the NIR we constructed a specific electronic setup consisting of a laser system with interchangeable laser diodes with different wavelength NIR light, a thermally-insulated cuvette-holder compartment with temperature measuring probes and a NIR spectrometer to control the stimulated fluorescence emission of the nanoparticle solutions. The temperature measurement compartment with the thermal-insulated cuvette holder was designed to maintain the solutions’ temperature at a fixed value right before the moment of laser irradiation. To maintain the measurement setup at a fixed temperature before the irradiation we used a thermal stabilized system based on two Peltier cells with electronic temperature control. The temperatures of the ambient air and the temperature of the cuvette walls were continuously measured in order to make corrections about the temperature dissipation during the irradiation.*

**Keywords:** light-to-heat conversion, gold nano-rods, gold nano-urchins, Peltier cell, Near Infrared measurements

## Introduction

Nanomaterials become more and more popular in modern medicine. Indeed, an entirely new division called nanomedicine, emerges with the latest introduction of new nanotechnologies in medical diagnostic and therapeutic applications [1 – 4]. Having dimensions from a nanometer up to several hundred nanometers nano-objects are comparable with many biological macromolecules, such as enzymes, antibodies, etc. Furthermore, compared to the same-substance normal size objects, nanomaterials exhibit different physical and chemical properties and open the prospective to a number of applications in various areas of biology and medicine [5 – 7]. In addition, properties of the nano-sized objects such as optical, electromagnetic, electronic, electroacoustic, etc., in combination with their specific spatial structure and composition are very promising for a wide range of biomedical applications such as cellular imaging, molecular diagnosis and targeted therapy [8].

Among the number of nanoparticles in use in the modern nanomedicine a particular class of objects, consisting of a noble metal, reveals an extreme sensitivity to the electromagnetic waves, due to the unique phenomenon of surface plasmon resonance (SPR). The small size of the conductive noble nanoparticles, often called plasmonic nanoparticles, results in a photon confinement in the small particle size, increasing thus all the radiative and nonradiative properties of the nanoparticles [9,10] and makes them ideal candidate for a number of biological and medical applications [11 – 13]. In this respect, the most promising nano-objects at present are the gold nanoparticles (GNP). These kinds of nano-objects unveil a number of excellent properties such as simplified synthesis and facilitated surface modification with a possibility to tune their plasmonic resonance parameters and hence to control important properties such as optical fluorescence emission, light-to-heat conversion, etc. Moreover, GNP are characterized as excellent biocompatible objects, feasible for biological applications and clinic settings.

The recent progress in the synthesis of GNP results in a great abundance of different shapes and structures [14] comprising gold nano-rods [15 – 16], hollow GNP [17], gold nano-urchins [18], etc. Important characteristic of all these particles is the size-dependence of their emission properties, which make possible a large red shift in their fluorescence properties, encouraging thus their use in applications such as molecular NIR imaging [19,20]. The enhancement in their absorption and scattering properties makes them extremely candidates for targeted photothermal cancer-cell destruction [21, 22] in particular and in general for photothermal cancer treatment and therapy [23 – 24].

The surface plasmon resonance in GNP is a phenomenon that creates very strong electromagnetic fields on the particle surfaces which results in the enhancement of their absorption and scattering of the electromagnetic waves. The quantity of the electromagnetic energy absorbed thus by the particle is quickly converted to heat via a series of nonradiative processes and consequently is dissipated in the surrounding media. In the Laboratory for Radiopharmaceuticals and Molecular Imaging (LARIM) at the Legnaro National Laboratories (LNL) of the National Institute for Nuclear Physics (INFN) in Italy, we have directed our investigation toward GNP specifically sensitive to electromagnetic radiation in the near-infrared region (NIR). In order to study the photothermic properties of the solutions of gold nanoparticles in the NIR we designed an experimental setup consisting of a laser system with interchangeable laser diodes with different wavelength NIR light and a thermally-insulated cuvette-holder compartment with temperature measuring probes. A NIR spectrometer was also a part of the system to measure the stimulated fluorescence emission of the nanoparticles' solutions. The temperature measurement compartment with the thermal-insulated cuvette holder was designed to maintain the solutions' temperature at a fixed value before the irradiation. The temperatures of the ambient air (the air temperature of the laboratory) and the temperature of the cuvette walls were continuously measured in order to make corrections about the temperature dissipation during the irradiation. In this article we present the design and realization of the experimental setup to conduct the light-to-heat measurements of solutions of GNP.

## Materials and Methods

A block-diagram of the measuring setup for the light-to-heat conversion of aqueous solution of GNP is shown in fig. 1. It is compounded by an excitation laser with a certain NIR wavelength, situated in a laser compartment, a power meter to measure the intensity of the laser beam after the transmission in the sample, a cuvette holder with a thermostatic system for control and maintenance of the temperature of the liquid in the cuvette. There is also a NIR spectrometer with the light guide to measure the fluorescence emission of the GNP solution. To ensure a stable work of the spectrometer we have placed it in a homemade thermostatic chamber, controlled by a PC. The intensity of the laser beam during the irradiation is maintained at a certain value by a special DC power supply block (THORLABS, model LDC 205C), and it has also temperature stabilization ensured by another block (THORLABS, model TED220C). The finest laser-beam intensity adjustment is achieved using a circular neutral variable filter (Newport circular variable metallic ND filter, model 50G02AV).

The power meter (THORLABS PM100 USB) and the InGaAs Hamamatsu C9406GC NIR spectrometer are connected to and operated by the PC using dedicated software supplied by the corresponding manufacturers. The temperature of thermally insulated cuvette holder and of the cuvette itself was maintained at a certain value using two Peltier cells with air cooling. Four temperature probes were used to control the temperature (fig. 1): probe  $S_1$  and probe  $S_4$  are to measure the temperature of the cuvette walls and the

temperature of the liquid with GNP; probe  $S_2$  measures the temperature of the NIR spectrometer compartment and probe  $S_3$  measures the temperature of the ambient air. To maintain the temperature of the GNP solution before the irradiation and to control it during the laser beam irradiation we modified the basic electronic setup used for the long-time constant-temperature storage measurements of single-walled carbon nanotubes (SWCNT) [25]. A specially developed in the Laboratory software, written in LabVIEW 8.2 and installed on a Windows-based PC with National Instruments board PCI 6025E [25], ensures the temperature measurement and maintenance of the thermally insulated cuvette holder, of the solution in the cuvette, as well as of the NIR spectrometer compartment. A constructed in the Laboratory hardware card, controlled by a PID algorithm [26], operates the current in the two Peltier cells installed on the outer surfaces of the chamber. In the same way another circuit, identical to the one described above, controls and maintains the temperature of the NIR spectrometer. A direct connection between the laser compartment and the computer was made to disable the thermostatic chamber temperature maintenance until the moment when the laser source is switched on, so that the increase of the temperature of the GNSU solution, read by the sensor in immersion, is not influenced.

The characterization of the NIR light-to-heat conversion of GNP in aqueous solutions is carried out measuring the temperature of the liquid as a function of time of irradiation with NIR laser diodes at different wavelength. Before the measurements at given wavelength a measurement of the laser beam intensity (power) is carried out without cuvette, with an empty cuvette and with a cuvette with GNP solution in order to calculate the absorbed energy in the liquid. For all measurements at different wavelengths, before each irradiation the temperature of the GNP solution is to be adjusted by the system to initially fixed value using the program for temperature adjustment and maintenance. The later insures the property that al the measurements are conducted at equal experimental conditions. The irradiation starts once the temperature of the liquid is achieved. The temperature maintenance program stops when the laser is on. The computer program makes a record of the four temperatures, measured by the probes  $S_1 - S_4$  in time intervals of 1 second. The program continues the temperature registration of about 5 minutes after the laser is off in order to measure the temperature dissipation of the cuvette with the GNP solution. NIR fluorescence emission spectra can also be made at the end of the 5 minutes' time interval measurements. After that, the temperature maintenance program starts the temperature adjustment and stabilization of the cuvette holder for the next irradiation measurement.

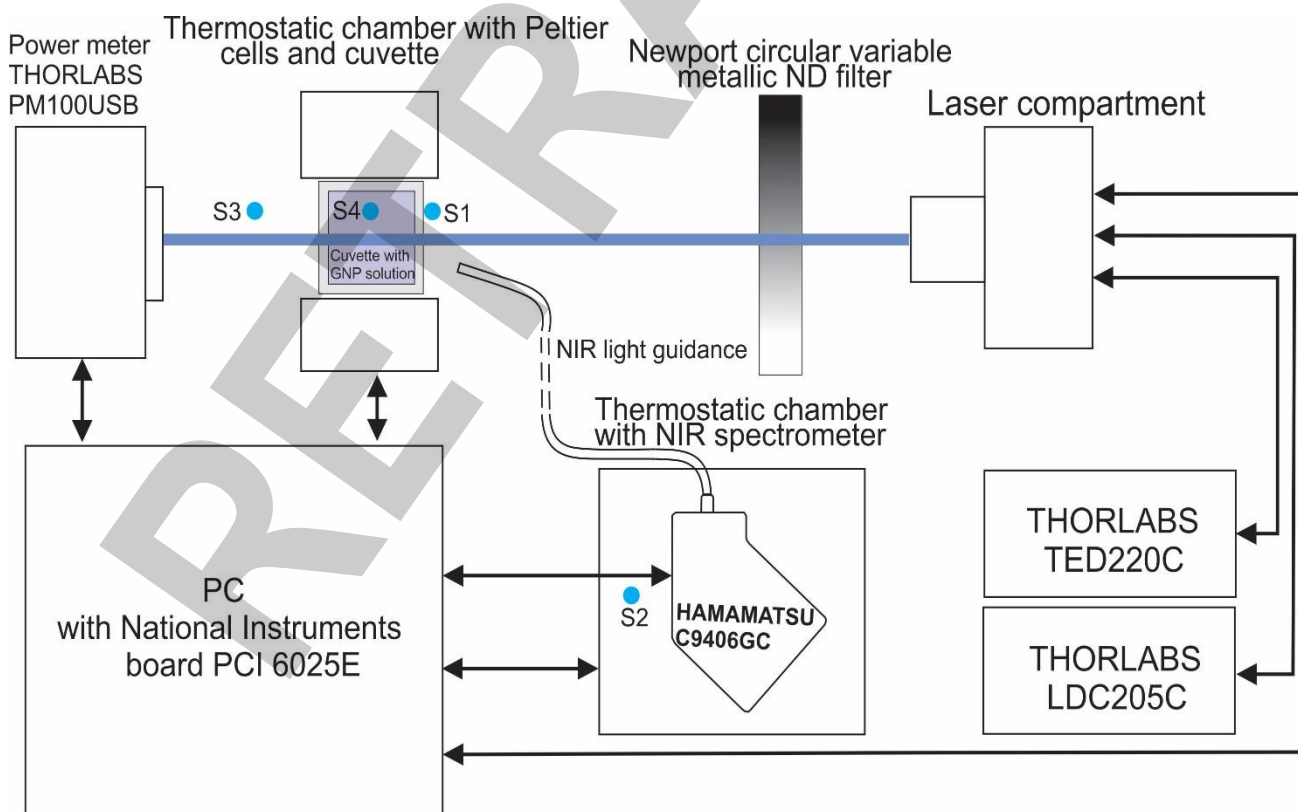


**Fig. 1.** Block diagram of the experimental setup for light-to-heat conversion measurements of aqueous solutions of GNP

### Experimental setup

The whole measuring system is compounded by the following elements:

1. A PC which runs a software written in LabVIEW 8.2 by National Instruments;
2. A plugged in PC National Instruments board PCI 6025E that communicates with ours developed hardware cards as well as with the temperature sensors;
3. Two constructed in the laboratory hardware cards on the basis matrix board composed by the 16F876A PIC microcontroller from Microchip, from a driver (a chip Tc4469 of Microchip) and a MOSFET (a IRLI 3705N of International Rectifier IOR, able to drive the current in the Peltier cell). Inside of the microcontroller is a module for Pulse Width Modulation (PWM) [26], One of these boards controls the temperature of the thermostatic chamber while the other controls the spectrometer compartment temperature;
4. Four temperature sensors LM35 TEXAS INSTRUMENTS, with corresponding signal amplifiers, one for thermostatic chamber, one for spectrometer, one for room temperature and the last one for temperature of the solution;
5. Three power supplies TTi EL302RT used to power the hardware cards and the amplifiers of the temperature sensors;
6. A thermostatic chamber made of aluminum, insulated with polystyrene of 1 cm and provided with two Peltier cells (Global Component Sourcing ET-127-14-15) complete with heat sink and fan;
7. A humidity sensor Honeywell HIH-5030 with its power supply;
8. Several THORLABS NIR laser diodes with different characteristics and wavelength as shown in Table 1.

**Table 1.** Characteristics of the laser diodes used to measure the light-to-heat NIR conversion of gold nanoparticles' solutions

Laser diode type	Wavelength (nm)	Pmax (mW)	Imax (mA)
HL7001MG	705	40	100
L785090	785	90	160
M9-808-0100	808	100	150
L820P100	820	100	210
M9-830-0159	830	150	220
L840P200	840	200	340
L850P200	850	200	340
L880P010	880	10	50
L904P010	904	10	70

Block diagram in Fig. 2 shows the interaction of the functional blocks of the system with their connections. The red connections represent the power supply lines. The celestial lines indicate sensor signals. The green ones are the amplified signals from the temperature sensors as well as the signals from the two control hardware cards, while the orange links represent the currents of the Peltier cell signals. With a violet is indicated the digital signal that drives the relay to reverse the Peltier cells' power supply mode. The latter is necessary when the Peltier cells are to switch from heating to cooling and vice versa.

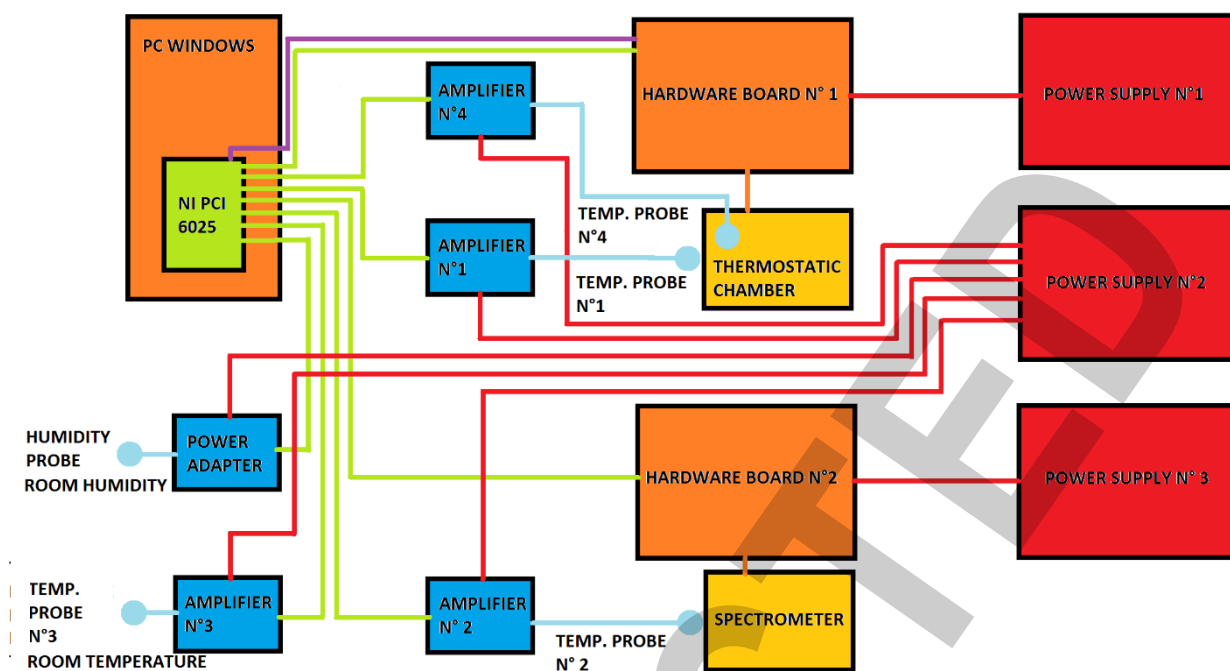


**Fig. 2.** Block diagram of the electronic setup for long-time constant-temperature maintenance of the thermostatic chamber

Software written in LabVIEW 8.2 controls the whole system. It reads the four temperature sensor signals as well as the humidity sensor signal through one 12-bit ADC (present in NIPCI6025 tab). It operates the hardware circuits by means of the DAC output channels 12 bits of NIPCI 6025, and realizes the two PID temperature controls. The software also performs a visualization of the measured values in run-time mode and finally saves the values of the four temperatures and the humidity as a function of time.

The program is formed by a continuous loop which is executed every 100 ms, a time more than sufficient to properly control the slow variations of the temperature. Before running the loop the program makes a variety of settings related to the initial conditions of the variables involved and also sets the analog channels and the name and location of the data files. Inside the loop the temperature and humidity sensors are read, the variables of the two PID controls are calculated and their output variables are updated, then the data are saved in a file and after that the graphics in the front panel are displayed. After the loop, which can only be closed by the front panel, the settings of the analog channels are reset and the data file is closed. In parallel a second loop of two seconds manages the inversion of the current in the Peltier cells of the thermostatic chamber, imposing heating or cooling according to the temperature value to be maintained. The inversion is automatically controlled by the value of the PID algorithm output: when this numeric value falls below -0.5 the current is reversed, the integral of the PID is reset and the control cycle restarts. These two modes are implemented at the hardware level through the switching of a relay that reverses the current in the Peltier cells (see the electrical scheme in fig 3 of [25]).

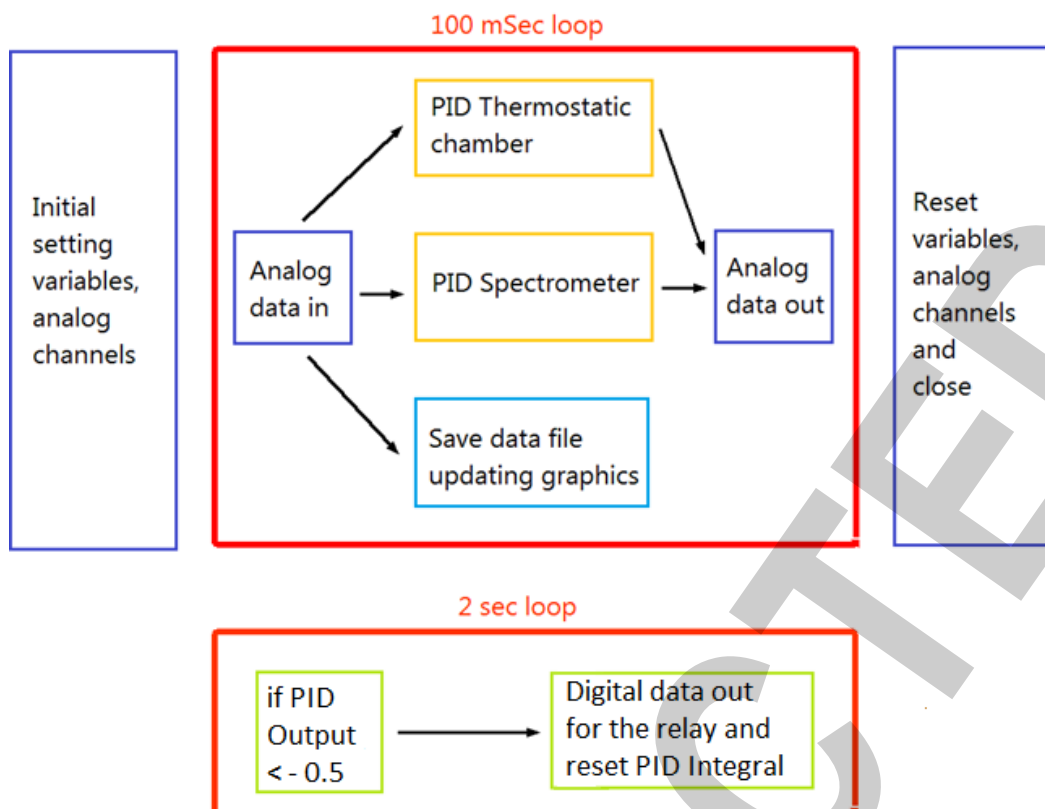


**Fig. 3.** Block diagram of the software for temperature control and temperature regulation

*The National Instruments board NI PCI 6025E*

This card through the PCI bus of the PC allows us to interface the analog and digital signals from the outside with the LabVIEW software. It has the ability to manage different signals: up to 8 differential analog inputs 12-bit, two 12-bit analog outputs, 32 digital inputs/outputs, and two 24-bit counters/timers. It uses a single ADC with sampling/rate maximum of 200Ks/s and a DAC with sampling/rate maximum of 10ks/s. For our application we used 5 differential analog inputs (temperature and humidity sensors), two analog outputs (control hardware cards) and two digital signals: one for control of the relay, inversion of the current in Peltier cells for the thermostatic chamber and another one to read if the laser is on or off.

*Hardware board for control of the temperature of the thermostatic chamber and of the NIR spectrometer*

Two hardware boards have been constructed in our laboratory to command adequately the current in the Peltier cells of the thermostatic chamber and to control the temperature of the spectrometer (see fig. 3 in [25]). The construction of these cards has been necessary both to be able to control, at the hardware level, the cell current in PWM (Pulse Width Modulation), and to eliminate the problems of thermal dissipation in the power consuming MOS-FET element. Another motive was to disengage the need to generate the PWM signal directly from the LabVIEW software, already busy in various other processes.

*Amplifiers of the temperature sensor signals and the humidity sensor power supply circuit*

The complete system uses four integrated temperature sensors LM35 of Texas Instruments. These devices offer an accuracy of  $\pm 0.4^{\circ}\text{C}$  throughout the operation range of  $-55$  to  $150^{\circ}\text{C}$ . However, for the temperature range used by our system (from  $5$  to  $50^{\circ}\text{C}$ ) the typical error is reduced to a maximum of  $\pm 0.1^{\circ}\text{C}$ , that is more than sufficient for our application (see fig. 4 in [25]).

For the humidity sensor (Honeywell HIH-5030) we used an application circuit recommended by the manufacturer (see fig. 5 in [25]). It was chosen to power supply the sensor with  $3.3\text{ V}$  from a voltage regulator

LM317 of the National Semiconductor. The output of the sensor (in Volts) is corrected by the written LabVIEW program using the equation described in [25].

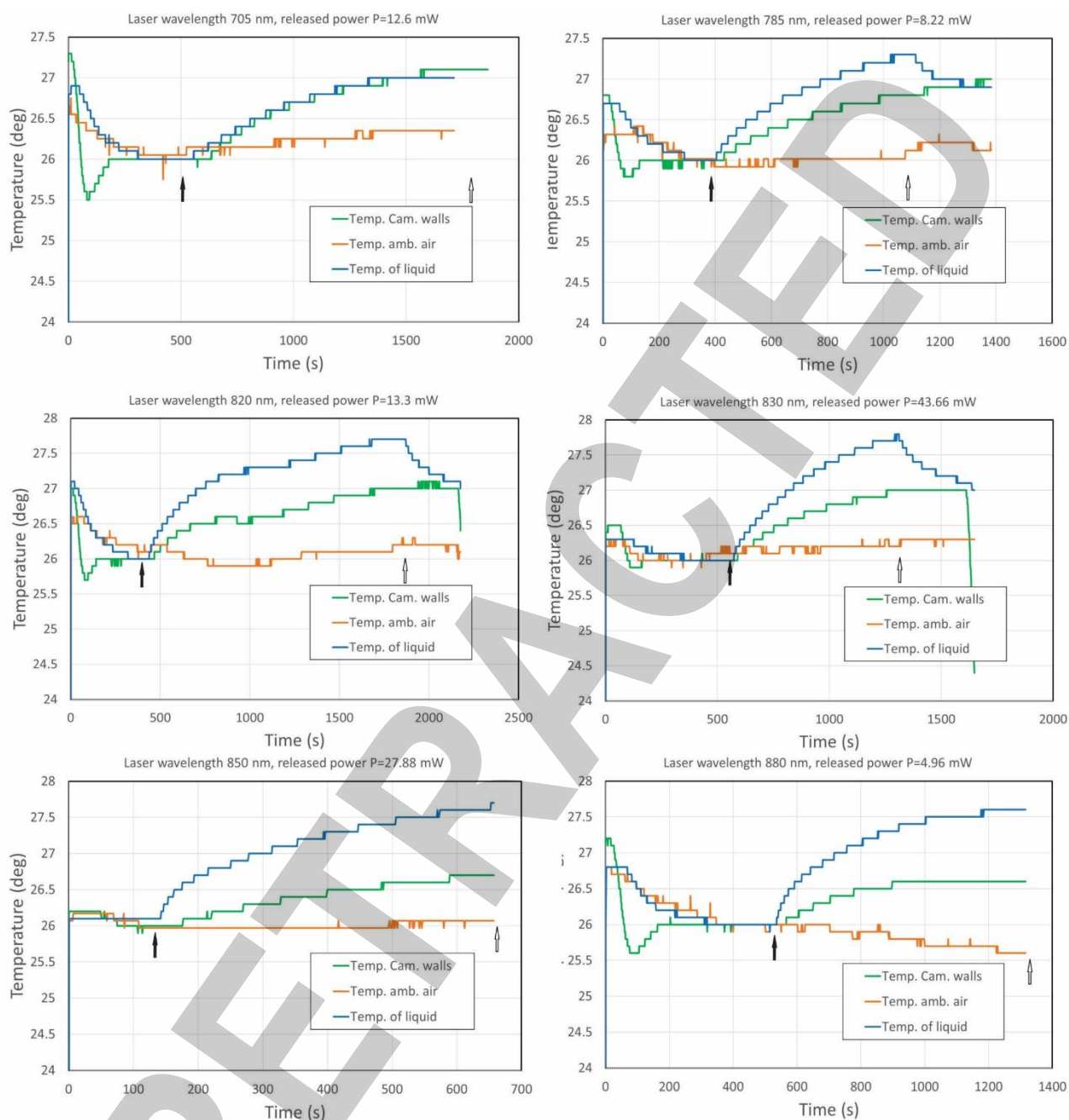


**Fig 4.** Measured temperatures of solution of gold nano-rods (blue line), of the cuvette's walls (green line) and of the ambient air (brown line) as a function of the time for 6 different laser wavelengths at different released power in the solution. The black arrows indicate the moments when the laser was on and the hollow arrows indicate the end of irradiation.

## Results

Test measurements on light-to-heat NIR conversion were carried out for several wavelengths. A quantity of 1 mL gold nano-rods dispersion in water, produced by SIGMA-ALDRICH (MERCK) was filled in a quartz cuvette. The average diameter of the nanoparticles was 10 nm and expected absorption wavelength 97

Corresponding author: nikolay.uzunov@lnl.infn.it

maximum was around 850 nm. The cuvette was hermetically closed to prevent the evaporation of the liquid and placed in the cuvette holder. Six NIR lasers with wavelengths of 705nm, 785nm, 820nm, 830 nm, 850 nm and 905nm were used to irradiate the solution. The initial temperature of the liquid, maintained by the system before the irradiation was 26<sup>0</sup> C. The temperature data of the solution, obtained from the immersed probe S4, of the quartz cuvette, obtained using S1 and the temperature of the ambient air, read by S3 probe were continuously recorded. The irradiation with the NIR light continued until the temperature of the solution changed with 1<sup>0</sup> C.

Figure 4 shows plots of the three temperatures measured during the irradiations, made for six NIR wavelengths. With black arrows are indicated the moments when the laser was on and the hollow arrows indicate the end of the irradiation. We exploited the power differences of the NIR diodes (see Table 1) in order to check the sensitivity of the temperature probes and to test how the temperature of the liquid differs from the one of the cuvette walls.

The damped sine wave behavior of the temperature of the cuvette walls in the beginning of each graph (the green line) reveals the work of the PID algorithm for the temperature adjustment in the thermostatic chamber compartment. One can clearly see the temperature increase of the nano-rods' solution following immediately the start of the irradiation (the black arrows) after the laser was on and the temperature decrease due to the heat dissipation after the hollow arrows, shown in the graphs.

In figure 4, one can see the strong evidence about the difference in the light-to-heat conversion effect at different wavelengths. The time needed to heat up the liquid with 1.5 <sup>0</sup>C (from 26 <sup>0</sup>C to 27.5 <sup>0</sup>C) for the laser wavelengths 830 nm, 850 nm, and 880 nm is around 500 seconds, while the released in the liquid powers are correspondingly 43.66 mW, 27.88 mW and 4.96 mW. For accurate quantitative calculations one should take into account the absorption of the cuvette's quartz walls and the absorption in the water. Since this material is characterized by its very low and extremely flat absorption region from 180nm up to 3000nm an eventual effect of heating should result in equal temperature increase at each used wavelength range. The absorption coefficients of NIR in water at 700 – 900 nm gradually increase [27]. If the effect of the liquid heating was due to the absorbed laser beam energy in water, we should have seen a gradual decrease of the heating time with the wavelength. Our observations however, demonstrate a more pronounced maximum of the liquid heating at about 880 nm followed by a decrease at 907 nm.

## Conclusions

We have designed and constructed a setup for light-to-heat NIR conversion measurements of gold nanoparticles' solutions. The whole setup was mounted and tested in the Laboratory for Radiopharmaceuticals and Molecular Imaging (LARIM) at the National Laboratories of Legnaro, INFN, Italy.

The specific conditions for temperature maintenance of the measuring thermostatic chamber before the laser irradiation and the need for precise temperature measurement of the GNP solution required a very thorough approach in the search and implementation of the electronic blocks and circuits. In addition, the special requirements for stability, reliability and fire safety as well as the requirements for protection against overloads and short circuits necessitated the construction of a system with much more specific capacities and capabilities. Exploiting the opportunities offered by the specialized boards such as the National Instruments board NI PCI 6025E to control and operate all the processes, implementing an appropriate software written in LabVIEW 8.2, it was possible to realize such a system.

Repeatability tests and other real time measurement tests on other GNP solutions with this system have already been carried out so far using the whole set of NIR lasers (see Table 1) available in the Laboratory. The system demonstrated excellent stability and reliability and proved that is suitable to conduct the light-to-heat NIR conversion measurements combined also with fluorescence emission studies of different solutions of gold nanoparticles.

## References

- [1] Abeer, S., Future Medicine: Nanomedicine, *JIMSA*, **2012**, 25 No. (3), 187 – 192
- [2] Freitas, R. A., What is nanomedicine?, *Nanomedicine*, **2005**, 1 (1), 2 – 9.
- [3] Sadanandam, N., Nanomedicine – the basis, *The West London Medical Journal*, **2011**, 3 (3), 11 – 14

- [4] Ranganathan, R.; Madanmohan, S.; Kesavan, A.; Baskar, G.; Krishnamoorthy, Y. R.; Santosham, R.; Ponraju, D.; Rayala, S. K.; Venkatraman, G., Nanomedicine: towards development of patient-friendly drug-delivery systems for oncological applications, *Int. J. Nanomedicine*, **2012**, 7, 1043 – 1080
- [5] El-Sayed, M.A., Some interesting properties of metals confined in time and nanometer space of different shapes, *Acc Chem Res*, **2001**, 34(4), 257 – 264.
- [6] Borzabadi-Farahani, A.; Borzabadi, E.; Lynch E., Nanoparticles in orthodontics, a review of antimicrobial and anti-caries applications, *Acta Odontologica Scandinavica*, **2014**, 72 (6), 413 – 417
- [7] Allen, T. M.; Cullis, P. R., Drug delivery systems: entering the mainstream, *Science*, **2004**, 303 (5665), 1818 – 1822.
- [8] Nie, S.; Xing, Y.; Kim, G. J.; Simons, J. W., Nanotechnology applications in cancer, *Ann Rev Biomed Eng*, **2007**, 9, 257 – 88.
- [9] Link S., El-Sayed M. A., Shape and size dependence of radiative, non-radiative and photothermal properties of gold nanocrystals, *Int Rev Phys Chem*, **2000**, 19(3), 409 – 53.
- [10] Link S., El-Sayed M. A., Spectral properties and relaxation dynamics of surface plasmon electronic oscillations in gold and silver nanodots and nanorods. *J Phys Chem B*, **1999**, 103(40), 8410 – 8426.
- [11] Huang X., Jain P. K., El-Sayed I. H., El-Sayed M. A., Gold nanoparticles: interesting optical properties and recent applications in cancer diagnostics and therapy, *Nanomed*, **2007**, 2(5), 681 – 693.
- [12] Skrabalak S. E., Chen J., Sun Y., Lu X., Au L., Cobley C. M., et al., Gold nanocages: synthesis, properties and applications, *Acc Chem Res*, **2008**, 41(12), 1587 – 1595.
- [13] Jain P. K., Huang X., El-Sayed I. H., El-Sayed M. A., Noble metals on the nanoscale: optical and photothermal properties and some applications in imaging, sensing, biology and medicine, *Acc Chem Res* **2008**, 41(12), 1578 – 1586.
- [14] Xia Y., Halas N.J., Shape-controlled synthesis and surface plasmonic properties of metallic nanostructures, *MRS Bull*, **2005**, 30(5), 338 – 43.
- [15] Yu Y. Y., Chang S. S., Lee C. L., Wang C. R. C., Gold nanorods: electrochemical synthesis and optical properties, *J Phys Chem B*, **1997**, 101(34), 6661 – 6664.
- [16] Murphy C. J., Sau T. K., Gole A. M., Orendorff C. J., Gao J., Gou L., et al., Anisotropic metal nanoparticles: synthesis, assembly and optical applications, *J Phys Chem B*, **2005**, 109(29), 13857–13870.
- [17] Sun Y., Mayers B. T., Xia Y, Template-engaged replacement reaction: a one-step approach to the large-scale synthesis of metal nanostructures with hollow interiors, *Nano Lett*, **2002**, 2(5), 481 – 485.
- [18] Bakr O. M., Wunsch B. H., Stellacci F., High-Yield Synthesis of Multi-Branched Urchin-Like Gold Nanoparticles, *Chem. Mater.*, **2006**, 18 (14), 3297 – 3301, DOI: 10.1021/cm060681i
- [19] Sokolov K., Aaron J., Hsu B., Nida D., Gillenwater A., Follen M., et al., Optical systems for in vivo molecular imaging of cancer, *Technol Cancer Res Treat*, **2003**, 2(6), 491 – 504.
- [20] Loo C., Lin A., Hirsch L., Lee M. H., Barton J., Halas N., et al., Nanoshell-enabled photonics-based imaging and therapy of cancer, *Technol Cancer Res Treat*, **2004**, 3(1), 33 – 40.
- [21] Chen J., Wang D., Xi J., Au L., Siekkinen A., Warsen A., et al., Immuno gold nanocages with tailored optical properties for targeted photothermal destruction of cancer cells, *Nano Lett*, **2007**, 7(5), 1318 – 1322.
- [22] Huang X., Jain P. K., El-Sayed I. H., El-Sayed M. A., Determination of the minimum temperature required for selective photothermal destruction of cancer cells with the use of immunotargeted gold nanoparticles, *Photochem Photobiol*, **2006**, 82(2), 412 – 417.
- [23] Hirsch L. R., Stafford R. J., Bankson J. A., Sershen S. R., Rivera B., Price R. E., et al., Nanoshell-mediated near-infrared thermal therapy of tumors under magnetic resonance guidance, *Proc Natl Acad Sci USA*, **2003**, 100(23), 13549–13554.
- [24] Huang X., El-Sayed I. H., Qian W., El-Sayed M. A., Cancer cell imaging and photothermal therapy in the near-infrared region by using gold nanorods, *J Am Chem Soc*, **2006**, 128(6), 2115 – 2120.
- [25] De Rosa M., De Nardo L., Bello M., Uzunov N., Electronic setup for fluorescence emission measurements and long-time constant-temperature maintenance of Single-Walled Carbon Nano-Tubes in water solutions, *Acta Scientifica Naturalis*, **2017** Vol 4, No 1, 61-69,
- [26] Hart D., Power Electronics. McGraw - Hill. (2010).
- [27] Palmer K. F., Williams, D., Optical properties of water in the near infrared, *Journal of the Optical Society of America*, **1974**, 64, 8, 1107 – 1110.